

# Electromechanical Modeling beyond VHDL-AMS

Lars M. Voßkämper<sup>\*</sup>, André Lüdecke<sup>†</sup>, Michael Leineweber<sup>†</sup>, Georg Pelz<sup>†</sup>

<sup>\*</sup>Dolphin Integration GmbH, Bismarckstr. 142a, D-47057 Duisburg, Germany

<sup>†</sup>Gerhard Mercator-University -GH- Duisburg, Finkenstr. 61, D-47057 Duisburg, Germany

## Abstract

Analytical modeling for electromechanics sometimes requires features like the representation of bended structures, the inclusion of (moving) boundary conditions or spatial integrations and differentiations. All these points are currently not directly addressed in VHDL-AMS and other analog hardware description languages. This paper illustrates this, using the example of a capacitive pressure sensor. The behavior of the introduced model is verified with finite element analysis.

**Keywords:** pressure sensor; analytical modeling; circular diaphragm; touch mode; multi-domain simulation.

## 1 Introduction

Though we are very much in favor of VHDL-AMS, the main contribution of this paper is to show its deficiencies concerning analytical modeling of electromechanical systems. Our example, a surface micro-machined capacitive pressure sensor [3], requires polynomial approximations of bending lines, moving mechanical boundary conditions and spatial integrations. For these features a direct language support would be desirable, but is currently not available. Thus, this paper may give hints for future extensions of VHDL-AMS and other analog hardware description languages to describe mechanical and electromechanical components.

To give an idea what is behind the above features, we provide an implementation. Necessarily, this results in a considerable amount of software, which sets up the model equations from timestep to timestep. Two solutions are available to include the respective code into the simulation: the formulation in C or VHDL-AMS. Since VHDL-AMS (as well as other analog hardware description languages) is a modeling language rather than a programming language, we chose the C-variant.

## 2 Device Modeling

The basic principle of the investigated pressure element is that some external pressure deflects the upper

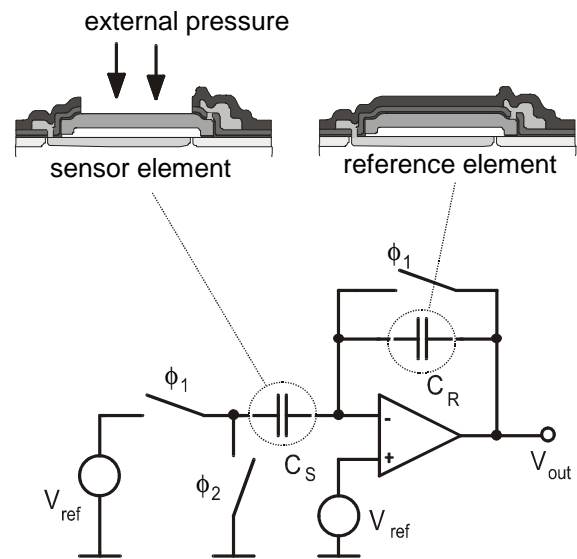


**Fig. 1: Basic sketch of capacitive pressure sensors with integrated readout electronics.**

plate of the sensor element which in turn leads to a change in its capacitance detected by the readout circuitry, see Fig. 1. The system behavior basically depends on the shape of the deflected upper plate, since it determines the pressure element's capacitance. Thus, the deflection has to be taken into account in a continuous way. For an accurate simulation, the following effects have to be taken into account:

- **touch mode**

In this case, the deflection of the diaphragm is that large that it touches the ground. This mode has several advantages in comparison with the non-touching mode: better linearity of the capacity to applied pressure, higher sensitivity, larger operating pressure range and large overload protection [6], [11], see Fig. 2. Some applications exploit this quality of the pressure element operating in this mode.

- **elastic clamped rim**

In common surface micromachined processes, the rim of a freestanding structure yields if the structure ex-

pired a mechanical load. This yielding could result in reasonable errors if this effect is not taken into account [7], [8].

- **electrostatic coupling**

The considering of the electrostatic coupling between a conductive mechanical structure and an electrical circuit leads to a multi-domain simulation. Since we want to do a homogenous simulation, we have to model the interaction between the electrostatic effect of an applied voltage and the mechanical bending of the diaphragm by ourselves [5].

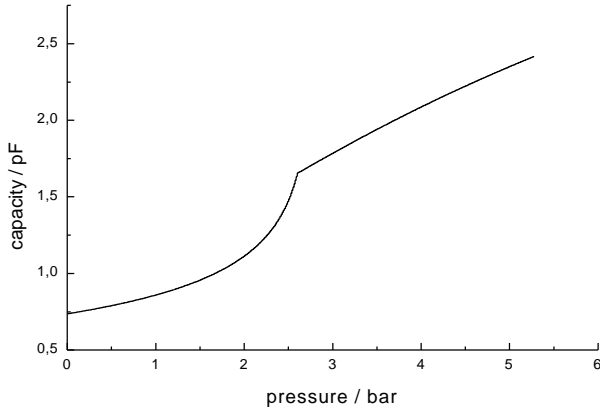


**Fig. 2: Capacity to pressure diagram of a pressure element. The diaphragm touches the ground at approximately 2.6 bar.**

The analytical modeling of the circular pressure element is to be performed on the basis of the following partial differential equation of fourth order [10]:

$$(1) \quad \Delta \Delta w = \frac{1}{D} (p + p_{el})$$

with the Laplace operator  $\Delta$ , the deflection  $w$ , the flexural rigidity of the plate  $D$ , the external pressure  $p$  and some electrostatic ‘pressure’  $p_{el}$ , which is due to the readout voltage.

The first challenge is to model the electrostatic pressure  $p_{el}$ . Some larger deflection leads to an increase of the electrostatic pressure which in turn results in an even larger deflection. This positive feedback has to be addressed carefully. The electrostatic pressure is defined as shown below.

$$(2) \quad p_{el}(r) = \frac{1}{2} \varepsilon \left( \frac{V}{d - w(r)} \right)^2$$

with the dielectric constant  $\varepsilon$ , the readout voltage  $V$ , the radius  $r$ , the deflection  $w$  and the distance  $d$  between the undeflected plate and the ground, see Fig. 3 and Fig.

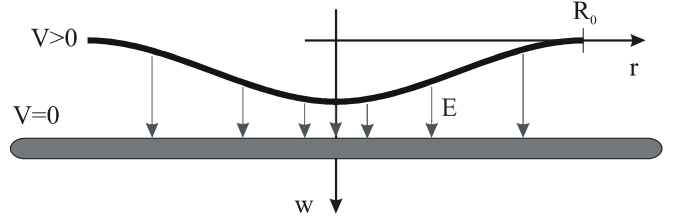


**Fig. 3: Bending line of plate before touching the ground with the electrical field  $E$  due to a readout voltage  $V$ .**

4. Solving for the deflection  $w$  in equation (1) leads to a sequence of four integrations over the radius. Thus, it is indispensable to approximate the electrostatic pressure polynomially:

$$(3) \quad p_{el}(r) \approx P_n(r) = \sum_{i=0}^n A_i r^i$$

This has to be carried out for any change of voltage and deflection caused by the external gas or fluid pressure  $p$  to be measured. After the coefficients  $A_i$  have been determined, the (Chebyshev) approximation greatly simplifies the analytical integration of equation (1) for its general solution:

$$(4) \quad w = \frac{1}{64 D} p r^4 + \frac{1}{4} C_1 r^2 \left( \ln \frac{r}{R_0} - 1 \right) + \frac{1}{4} C_2 r^2 + C_3 \ln \frac{r}{R_0} + C_4 + \sum_{i=0}^n \frac{A_i}{(i+2)^2 (i+4)^2} r^{i+4}$$

with the four integration constants  $C_1$  to  $C_4$  due to the four integrations of equation (1) and the radius of the circular diaphragm  $R_0$ . To determine these constants, we have to evaluate boundary conditions. In the non-touching mode, see Fig. 3, this can be done in advance, which leads to the final solution:

$$(5) \quad w = \frac{1}{64 D} p (R_0^2 - r^2)^2 + \frac{(R_0^2 - r^2)}{2D} \sum_{i=0}^n A_i \frac{R_0^{i+2}}{(i+2)^2 (i+4)^2} - \frac{1}{D} \sum_{i=0}^n A_i \frac{R_0^{i+4} - r^{i+4}}{(i+2)^2 (i+4)^2}$$

When solving for the bending line, we have to iterate, which is caused by the approximation of  $p_{el}$  in the differential equation (1). Any change of the deflection line requires a recalculation of the electrostatic pressure (2)

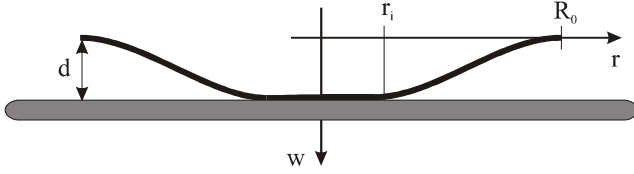


**Fig. 4: Bending line of plate after touching the ground with the touching radius  $r_i$ .**

and the Chebyshev approximation (3), which in turn modifies the deflection line (5). To solve this feedback, we have implemented some Gauß-Seidel relaxation.

In touch mode, see Fig. 4, a fifth unknown has to be accounted for: the touch radius  $r_i$ , which introduces moving boundary conditions, because the plate ‘rolls’ over the ground with increasing pressure. The governing boundary equations for this case are:

$$(6) \quad \begin{aligned} w|_{r=r_i} &= d, \quad \frac{\partial}{\partial r} w|_{r=r_i} = 0, \quad w|_{r=R_0} = 0, \\ M|_{r=R_0} &= kM_c|_{r=R_0}, \quad M|_{r=r_i} = 0 \end{aligned}$$

with  $M$  the radial torque of the plate with yielding rim and  $M_c$  the radial torque of the plate with clamped rim.  $k$  is a number representing the rim stiffness, its value is between 0 (plate with only supported rim) and 1 (plate with rigid clamped rim).

The resulting symbolic equation explodes in size. Thus we chose to calculate the constants  $C_1$  to  $C_4$  and  $r_i$  as numerical values from the governing equations and to insert them into equation (4). This has to be done anyway, since the boundary conditions are moving as the plate ‘rolls’ over the ground with increasing pressure. To implement this, we have to determine the zeros of the respective functions, using the iterative method of Newton.

Now, we have calculated the bending line of the plate, but the readout circuit requires the capacitance of the pressure element. Thus, we have to integrate over the radius to calculate the capacitance of the pressure element. Again, this cannot be formulated directly in an analog HDL. We decided to implement Simpson’s rule for that.

The model described above is implemented for SMASH, the mixed signal and multi-level simulator provided by DOLPHIN Integration<sup>1</sup>. The pressure sensor uses currently the Analog and Behavioral C-based Description namely ABCD<sup>2</sup> language. The model is by no means restricted to ABCD and could be written in VHDL-AMS as well as in almost any other analog hardware description language.

<sup>1</sup> DOLPHIN Integration S.A., Grenoble, France

<sup>2</sup> ABCD is implemented into SMAH. The LRM is available on [www.dolphin.fr/smash.html](http://www.dolphin.fr/smash.html)

### 3 System Simulation

Fig. 5 illustrates the simulation results of the pressure sensor system in Fig. 1, using the SMASH simulator. The first slot shows the voltage of an equivalent pressure rising from 0 to 0.4 bar (40000 Pa). The next one displays the clock of a readout voltage in the SC-circuit (low: 0V, high: 10V). The third trace shows the maximal deflection of the pressure sensor (0 to 0.8 $\mu$ m). The fourth trace represents the touch radius  $r_i$  (0 to 11.5 $\mu$ m). Finally, the fifth trace shows the capacitance of the sensor element (0.35pF to 1.1pF). The traces show the large influence of the readout voltage, especially if the two plates are close together.

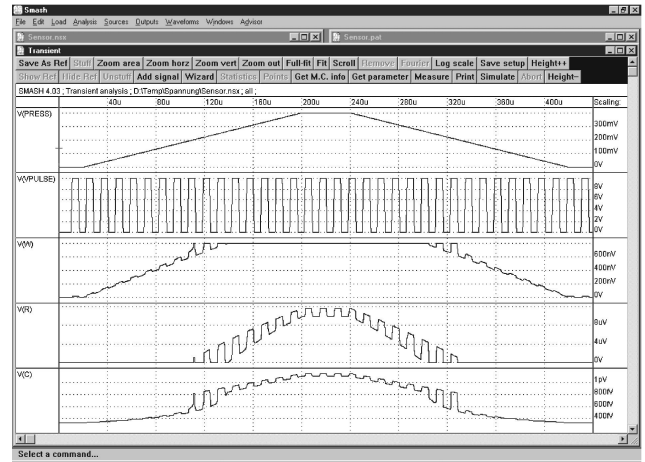


**Fig. 5: Simulation results of pressure sensor displayed in Fig. 1**

### 4 Model Verification

For the verification of the mechanical behavior, we obtained several bending lines for three different types of pressure elements (50 $\mu$ m, 70 $\mu$ m and 120 $\mu$ m in diameter). For these, the respective pressure range was covered by applying four pressure values. Fig. 6 - Fig. 8 compares the results to values obtained by the finite element simulator ANSYS<sup>3</sup>. The maximum difference is below 1% and indicating that the analytical results are at least as good as those accomplished by a fully-fledged finite element simulator.

<sup>3</sup> Ansys Inc., Houston, PA, USA.

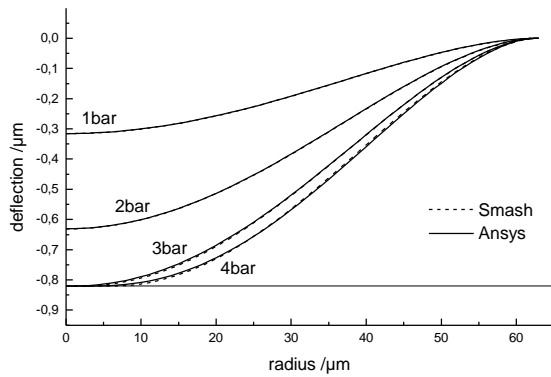


**Fig. 6: Bending lines for 120  $\mu\text{m}$  diameter pressure elements under several pressure conditions.**

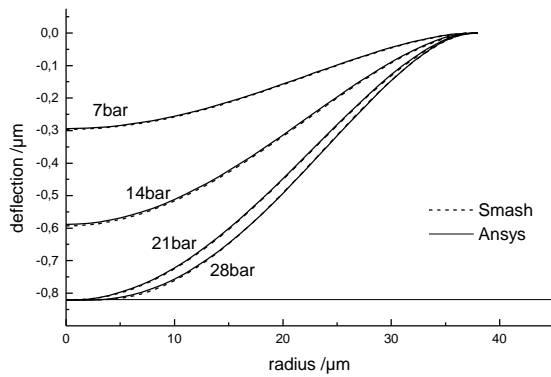


**Fig. 7: Bending lines for 70  $\mu\text{m}$  diameter pressure elements under several pressure conditions.**

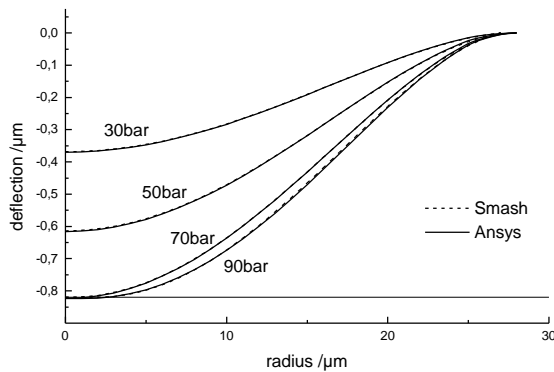


**Fig. 8: Bending lines for 50  $\mu\text{m}$  diameter pressure elements under several pressure conditions.**

## 5 Conclusion

VHDL-AMS and other analog hardware description languages currently allow to model mechanics. Unfortunately, some features are missing for some cases, e.g. the representation of bended structures, the inclusion of (moving) boundary conditions or spatial integrations and differentiations. For the extension of VHDL-AMS and the respective packages, it might be helpful to include the above features in one or the other way. Then one could concentrate on the set up of the model equations rather than worrying about implementing mathematical help-functions. Furthermore, the simulation speed and accuracy would become independent from the modeler's choice of help-functions.

## References

- [1] J. Bielefeld, G. Pelz and G. Zimmer, "AHDL-Model of a 2D Mechanical Finite-Element usable for Micro-Electro-Mechanical Systems", IEEE/VIUF Workshop on Behavioral Modeling and Simulation (BMAS), Washington D.C., 1997, 177-182.
- [2] X. Cai, P. Osterberg, H. Yie, J. Gilbert, S. Senturia, and J. White, "Self-Consistent Electromechanical Analysis of Complex 3-D Microelectromechanical Structures Using Relaxation/Multipole-Accelerated Method", Sensors and Materials 6 (1994) /2, 85-99
- [3] H. Dudaicevs, Y. Manoli, W. Mokwa, M. Schmidt and E. Spiegel, "A Fully Integrated Surface Micromachined Pressure Sensor with Low Temperature Dependence", Proc. Transducers 1995, 616-619.
- [4] G.K. Fedder, Q. Jing, "NODAS 1.3 - Nodal Design of Actuators and Sensors", IEEE/VIUF Workshop on Behavioral Modeling and Simulation (BMAS) 1998
- [5] A. Klein, A. Schroth, T. Blochwitz, and G. Gerlach, "Two Approaches to Coupled Simulation of Complex Microsystems", EUROSIM 1995, 639-644
- [6] G. Meng, and W.H. Ko, "Modeling of Circular Diaphragm and Spreadsheet Solution Programming for Touch Mode Capacitive Sensors", Sensors and Actuators A, 75 (1999), 45-52
- [7] Q. Meng, M. Mehregany, and R.L. Mullen, "Analytical Modelling of Step-Up Supports in Surface-Micromachined Beams", International Conference on Solid-State Sensors and Actuators 3 (1993)
- [8] R.L. Mullen, M. Mehregany, M.P. Omar, and W.H. Ko, "Theoretical Modeling of Boundary Conditions in Microfabricated Beams", Proceedings of the IEEE - MEMS 1991, 154-159
- [9] S.D. Senturia, N. Aluru, and J. White, "Simulating the Behavior of MEMS Devices: Computational Methods and Needs", IEEE Computational Science & Engineering, 4 (1997), 30-43
- [10] S.P. Timoshenko and S. Woinowsky-Krieger, "Theory of Plates and Shells", 27<sup>th</sup> Printing, 1987, McGraw-Hill.
- [11] Q. Wang, and W.H. Ko, "Modeling of Touch Mode Capacitive Sensors and Diaphragms", Sensors and Actuators A, 75 (1999), 230-241